

Field Verification of the Wind Tunnel Coefficients

W. K. Gawronski

Ground Antennas and Facilities Engineering Section

J. A. Mellstrom

Avionic Systems Engineering Section

Accurate information about wind action on antennas is required for reliable prediction of antenna pointing errors in windy weather and for the design of an antenna controller with wind disturbance rejection properties. The wind tunnel data obtained 30 years ago using a scaled antenna model serves as an antenna industry standard, frequently used for the first purpose. The accuracy of the wind tunnel data has often been challenged, since they have not yet been tested in a field environment (full-sized antenna, real wind, actual terrain, etc.). The purpose of this investigation was to obtain selected field measurements and compare them with the available wind tunnel data. For this purpose, wind steady-state torques of the DSS-13 antenna were measured, and dimensionless wind torque coefficients were obtained for a variety of yaw and elevation angles. The results showed that the differences between the wind tunnel torque coefficients and the field torque coefficients were less than 10 percent of their values. The wind-gusting action on the antenna was characterized by the power spectra of the antenna encoder and the antenna torques. The spectra showed that wind gusting primarily affects the antenna principal modes.

I. Introduction

The wind tunnel tests of antenna wind loading were conducted more than 30 years ago,^{1,2,3} and they serve as an antenna industry source for the determination of antenna pointing errors [1]. The wind tunnel results presented in Footnote 3, the CP-6 Memorandum, are considered the most reliable since the antenna model rather than the dish-only model (as in Footnotes 1 and 2) was used in the experiment, and the ground effects were accounted for. The wind tunnel model of the antenna in the CP-6 Memorandum had a reflector diameter of 0.46 m (18 in.), which gives a scale factor of 1 to 75 when compared with the DSS-13 reflector of 34 m. Holes were drilled in the reflector on the outer 25 percent of its radius to obtain a 25-percent porosity in that area. The CP-6 Memorandum presented two sets of data, "metric"

¹ N. L. Fox and B. Layman, Jr., "Preliminary Report on Paraboloidal Reflector Antenna Wind Tunnel Tests," JPL Interoffice Memorandum CP-3 (internal document), Jet Propulsion Laboratory, Pasadena, California, 1962.

² N. L. Fox, "Load Distributions on the Surface of Paraboloidal Reflector Antennas," JPL Interoffice Memorandum CP-4 (internal document), Jet Propulsion Laboratory, Pasadena, California, 1962.

³ R. B. Blaylock, "Aerodynamic Coefficients for Model of a Paraboloidal Reflector Directional Antenna Proposed for a JPL Advanced Antenna System," JPL Interoffice Memorandum CP-6 (internal document), Jet Propulsion Laboratory, Pasadena, California, 1964.

(alidade attached at the elevation bearing and not attached at the azimuth bearing) and “nonmetric” (alidade not attached at the elevation bearing and attached at the azimuth bearing). In this comparison, metric data were used (the difference between the two sets of data was within 10 percent).

The tunnel tests need verification, since they were run on small models of reflectors, as in Footnotes 1 and 2, or small models of antennas, as in Footnote 3, and they were conducted in wind tunnels where conditions are not necessarily the same as in the actual antenna environment. However, the repetition of such wind tunnel tests in the field would be a costly (expensive instrumentation) and time consuming (lack of controlled environment) procedure. Therefore, instead of a complex measurement of wind pressure distribution on the antenna structure, a simplified approach was chosen. It consisted of measuring elevation and azimuth torques generated by wind on the DSS-13 antenna and of comparing them with the torques obtained in the wind tunnel on the antenna model. The torques represented the summary wind loads on the antenna and thus served as the accuracy indicator of the wind tunnel tests.

In addition, wind gusting on the antenna was measured, with the gusting action characterized by the power spectra of the pointing error and the torques. The spectra reflected the frequency contents of the antenna response to the wind.

II. Torque Coefficients

Antenna torques due to wind depend on the antenna size, represented by the dish diameter, D ; wind velocity, v ; porosity of the antenna dish; the distance, d , of the dish vertex from the elevation axis (see Fig. 1); the elevation angle of the antenna, β_e ; and the wind direction with respect to the antenna dish, yaw angle β_a . By rescaling the torques, one can make the torques independent of antenna size and wind speed. These dimensionless and scaled torques, called torque coefficients, c_t , are defined in Footnote 1 as

$$c_t = \frac{T_w}{p_d A D} \quad (1)$$

where T_w is the on-axis torque, N-m (lb-ft); p_d is the dynamic pressure, N/m² (lb/ft²); A and D are the antenna dish frontal area, m²(ft²), and diameter, m (ft), respectively; and $A = \pi D^2/4$.

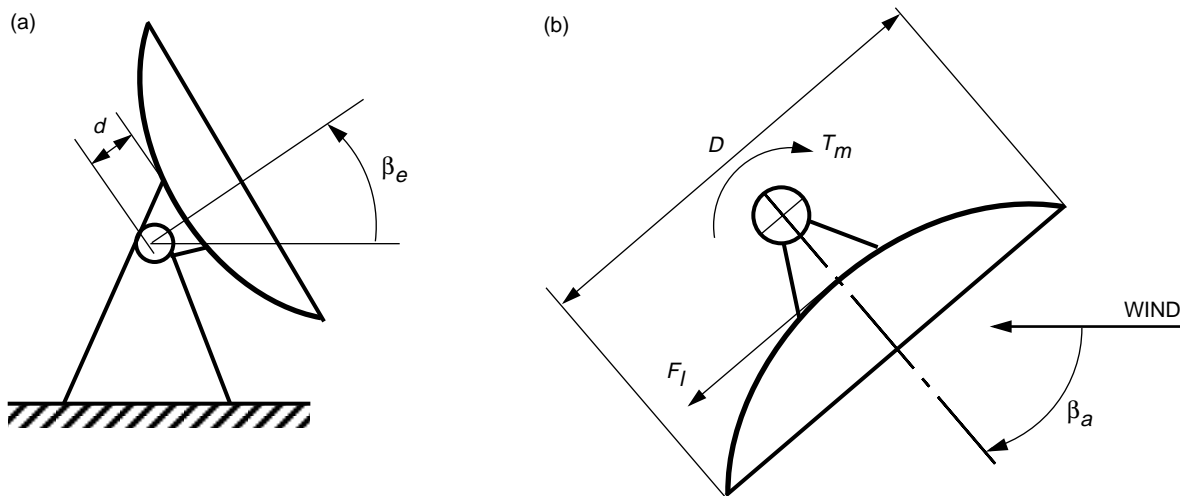


Fig. 1. Antenna configuration with respect to wind: (a) side view and (b) top view.

A. Obtaining Torque Coefficients From Field Data

The dynamic pressure depends on wind speed, v km/hr (mph), as follows:⁴

$$p_d = \alpha_p v^2 \quad (2)$$

where $\alpha_p = 0.0478$ (in SI units) or 0.00256 (in English units), and is illustrated in Fig. 2. For the 34-m antenna, $AD = 30,874 \text{ m}^3$ ($1.0903 \times 10^6 \text{ ft}^3$), which when combined with Eq. (2) gives Eq. (1) as follows:

$$c_t = \alpha_t \frac{T_w}{v^2} \quad (3)$$

where $\alpha_t = 6.7761 \times 10^{-4}$ (in SI units) or 3.586×10^{-4} (in English units), and T_w is in N-m (lb-ft) and v in km/hr (mph).

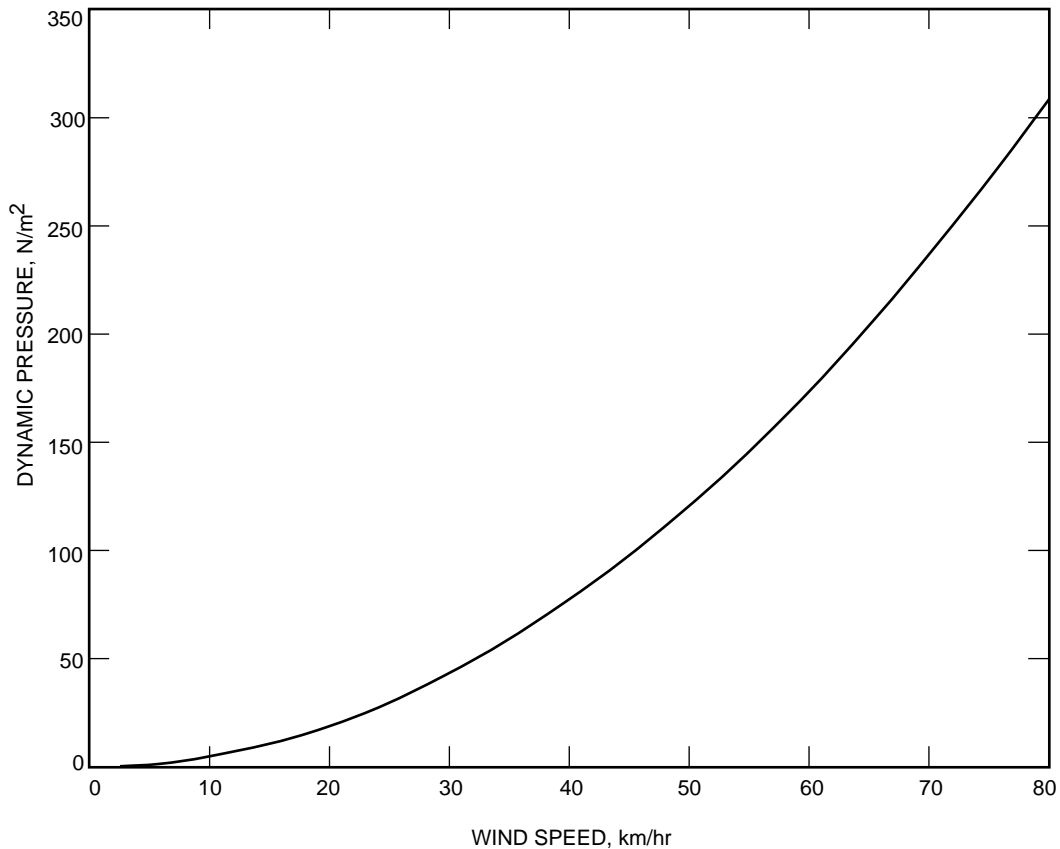


Fig. 2. Wind dynamic pressure on the antenna versus wind speed.

In the field, the torque was measured while slewing the antenna with the constant rate of 0.05 deg/sec . In this case, the measured torque, T_m , consisted of the torque generated by wind, T_w , and the friction torque, T_f ; thus,

$$T_w = T_m - T_f \quad (4)$$

⁴N. L. Fox and B. Layman, Jr., op. cit.

The friction torque, T_f , was measured when slewing the antenna with the same rate and with the wind speed close to zero. Hence, the torque coefficient from Eq. (3) is now

$$c_t = \alpha_t \frac{T_m - T_f}{v^2} \quad (5)$$

The torque coefficients depend on the porosity of the antenna dish; the distance, d , of the dish vertex from the elevation axis; the elevation angle of the antenna; and the yaw angle. The distance, d , has the same effect on the torque coefficients for the DSS-13 antenna and the CP-6 Memorandum model. To prove it, note that the total azimuth axial torque is a sum of the dish torque, T_d , and the torque, T_l , generated by the lateral force, F_l (see Fig. 1). From this figure, one obtains

$$T_l = F_l d \cos \beta_e \quad (6a)$$

or

$$c_{tl} = c_{fl} \cos \beta_e \frac{d}{D} \quad (6b)$$

where β_e is the elevation angle, c_{tl} is the lateral torque coefficient, and c_{fl} is the lateral force coefficient,

$$c_{tl} = \frac{T_l}{p_d A D}, \quad c_{fl} = \frac{F_l}{p_d A} \quad (7)$$

The ratio $d/D = 0.14$ for the CP-6 Memorandum case and 0.11 for the DSS-13 antenna; thus, they are close enough so that from Eq. (6b) it follows that the lateral force coefficient is about the same in the CP-6 experiment and the DSS-13 antenna experiment.

The porosity of the DSS-13 antenna dish is about 25 percent of the outer 25-percent radius, similar to the CP-6 model.

The torque coefficient was tested with respect to the two remaining “free” parameters: elevation angle, β_e , and yaw angle, β_a . Thus, the torque coefficient was a function of β_e and β_a , i.e., $c_t = c_t(\beta_e, \beta_a)$.

B. Fitting Wind Tunnel Results to the Field Data

In the following, the field and wind tunnel data were compared. The torque coefficients were obtained for the range of yaw angles, from 0 to 180 deg, with the elevation angle fixed; thus, $c_t = c_t(\beta_a, i)$, where i is the sample number. They were also measured for a range of elevation angles, from 10 to 89 deg, with the yaw angle fixed, so that $c_t = c_t(\beta_e, i)$. Denote the torque coefficient from the CP-6 Memorandum $c_{t6}(\beta_a)$ if it depends on yaw angle or $c_{t6}(\beta_e)$ if it depends on elevation angle. The new coefficients, c_{t6new} , are obtained as a linear combination of c_{t6} ,

$$c_{t6new}(\beta) = s_1 c_{t6}(\beta) + s_2 \quad (8)$$

where $\beta = \beta_a$ or $\beta = \beta_e$, and the coefficients s_1 and s_2 are determined such that the error, ε , between the CP-6 Memorandum and the field data,

$$\varepsilon(s_1, s_2) = \sum_{i=1}^n (c_t(\beta, i) - c_{t6new}(\beta))^2 \quad (9)$$

where $\beta = \beta_a$ or $\beta = \beta_e$, is minimal. The parameter s_1 is the scaling coefficient, and s_2 is the shifting coefficient. The parameter s_1 scales the CP-6 Memorandum curve c_{t6} to best fit the field data. The parameter s_2 shifts the field data to compensate for undetermined friction forces.

The windy data were collected on two days: January 24, 1994, and March 22, 1994. The sampling frequency was 40 Hz, and the antenna azimuth rate was 0.05 deg/sec. The wind speed ranged from 25 to 65 km/hr (15 to 40 mph). Rotating the antenna 360 deg in azimuth with a fixed elevation angle (at 10 or 60 deg), the azimuth torques were measured.

On March 22, 1994, the torques were measured for the average wind speed of 60 km/hr (37 mph) and an elevation angle of 10 deg. The wind direction was 251 deg with respect to the azimuth encoder zero position. The yaw angle is the difference between the antenna azimuth position and the wind direction. The plot of the azimuth torques versus yaw angle is shown in Fig. 3(a). The plots were obtained by averaging torques every 5 sec, and by subtracting the friction torque, which was measured for a non-windy day at 17.9 N-m (15.8 lb-ft). This plot is expected to be antisymmetric, and a small departure from the antisymmetry is caused by the varying wind speed during this experiment. The mean wind speed (a linear fit to the wind speed data) is shown in Fig. 3(b). By rescaling the torques according to Eq. (5), the torque coefficient was obtained (Fig. 4, dots). The CP-6 Memorandum torque coefficient was best fitted to this data (Fig. 4, solid line). It required scaling $s_1 = 1.016$ and shifting $s_2 = 0.0066$. That means that the wind tunnel data are less than 2 percent apart from the field data. The friction torque estimation is about 10 percent error, since the shift $s_2 = 0.0066$ corresponds to 1.8 N-m (1.6 lb-ft) friction torque. Two other experiments for an elevation angle of 10 deg required scaling of 1.07 and 1.11; thus, the accuracy of the tunnel data for this case can be considered to be less than 10 percent.

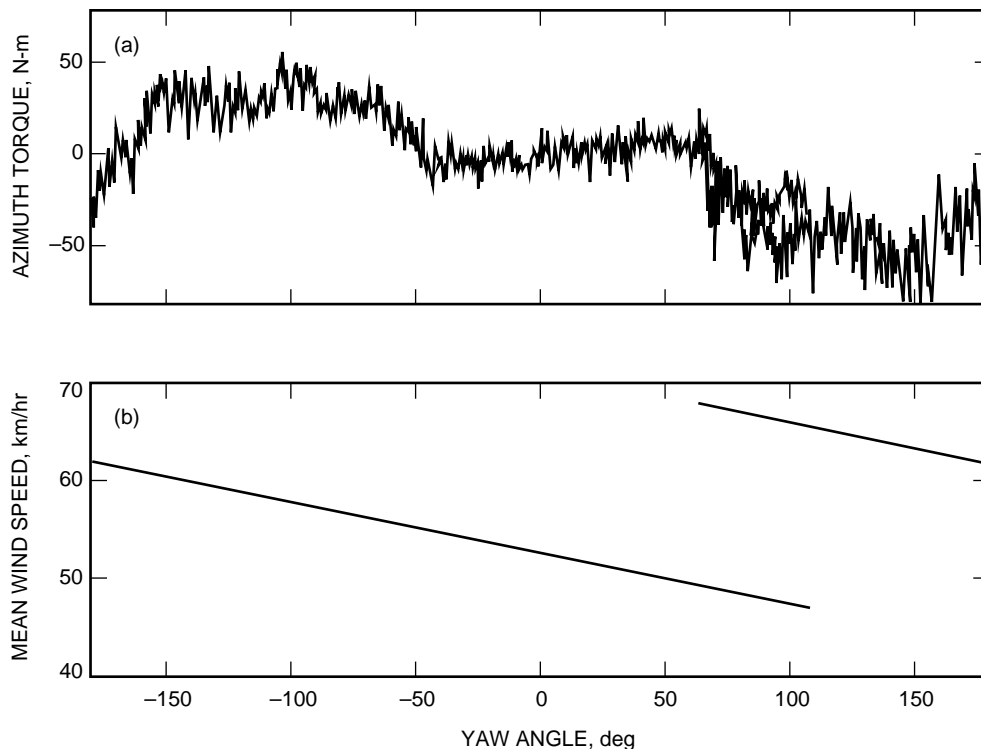


Fig. 3. Elevation angle 10 deg: (a) azimuth torque and (b) mean wind speed versus yaw angle.

A similar experiment was conducted on January 24, 1994, for an elevation angle of 60 deg. The averaged field-measured torques (dots) and CP-6 Memorandum data (solid line) are shown in Fig. 5. For this case, $s_1 = 1.08$ and $s_2 = 0.0008$; thus, the difference between the field and the CP-6 Memorandum data was within 8 percent, and the friction torque correction was about 1 percent.

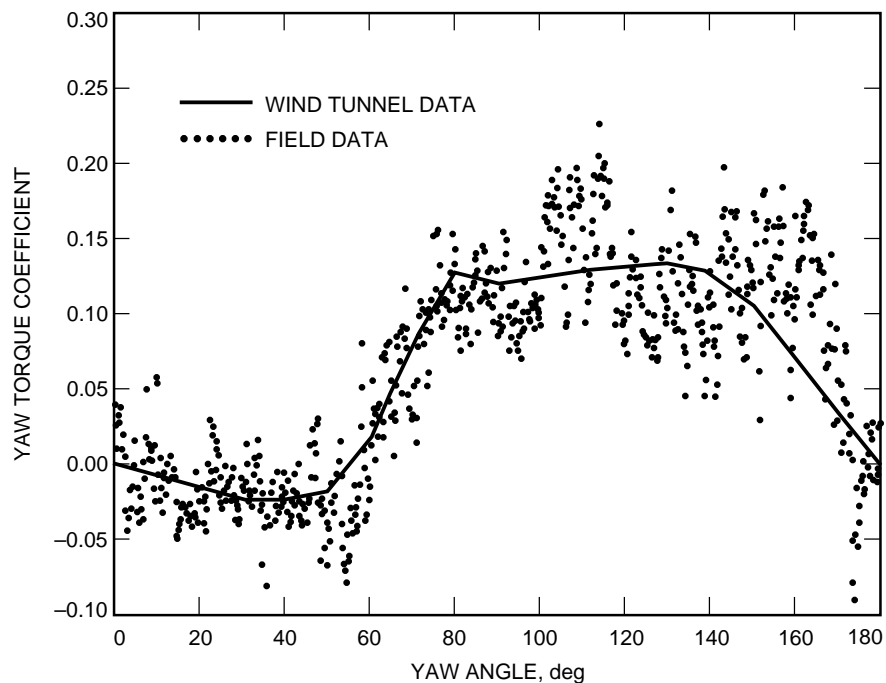


Fig. 4. Yaw torque coefficient from wind tunnel data and field data for elevation angle 11 deg.

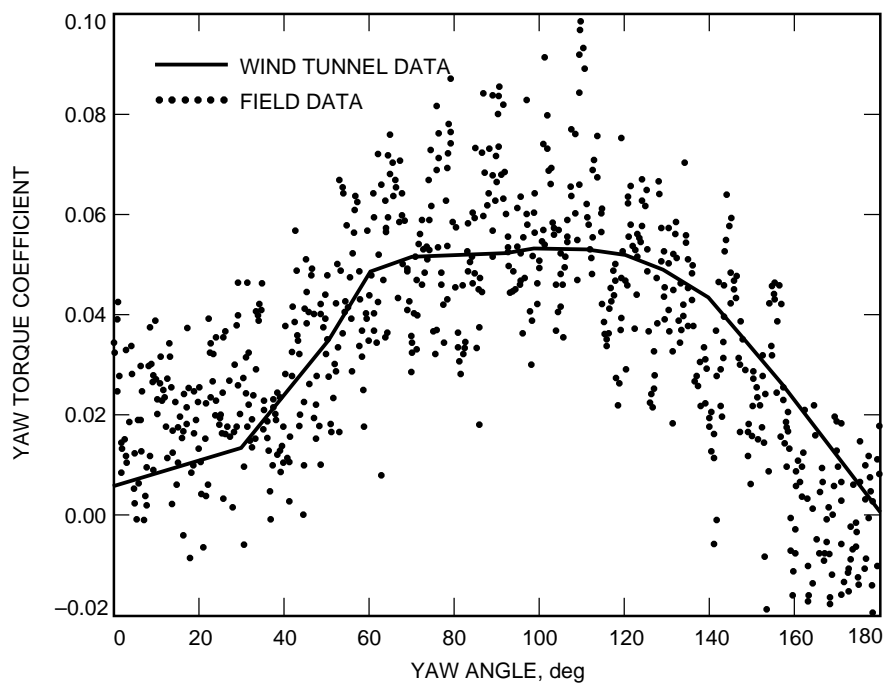


Fig. 5. Yaw torque coefficient from wind tunnel data and field data for elevation angle 60 deg.

The elevation (pitch) torque coefficients were verified for winds blowing from behind the antenna (a yaw angle of 180 deg). The torques were measured on January 24, 1994, for elevation angles ranging from 10 to 89 deg. The friction and unbalanced torques were obtained from Ahlstrom and Mellstrom.⁵ The friction torques are 5.2 N-m (4.6 lb-ft), and the unbalanced torques are 2.0 N-m (1.8 lb-ft), with opposite direction to the friction torques (the antenna dish was driven down). The torques are plotted in Fig. 6(a). These torques were scaled to obtain the torque coefficients, and the CP-6 Memorandum torque coefficients were fitted to the field data [see Fig. 6(b)]. The fitting coefficients were $s_1 = 0.87$, $s_2 = -0.013$, showing that the CP-6 and field measurements are within a 13-percent error margin. A slightly larger s_2 was due to poorer friction torque estimation (friction torques in Footnote 5 were obtained for different rates, and the unbalance torque was not known exactly).

III. Power Spectra Analysis

The torque coefficients characterize the wind steady-state pressure on the antenna. In order to have insight into the wind-induced dynamic of the antenna, the power spectra of the torques and the encoder output were obtained.

The resonance peaks in the spectra carry information about flexible modes excited by the wind. These modes can be identified from the elevation and azimuth closed-loop transfer functions of the antenna, shown in Fig. 7. The principal azimuth flexible-mode frequency is 1.66 Hz. Two other azimuth flexible modes are at 3.20 and 4.23 Hz. The principal elevation flexible-mode frequency is 1.95 Hz, and the other two are 3.16 and 5.18 Hz. The principal elevation mode is a bending mode of the antenna [2]. Note also that the second azimuth mode and the second elevation mode are probably the same one, because their frequencies are almost identical.

Figure 8 shows the power spectra of the azimuth encoder and azimuth torque for a 180-deg yaw angle (wind from behind the antenna), for elevation angle 10 deg, and for wind speeds 34 and 60 km/hr (21 and 37 mph). The plots show a dramatic increase of power spectra with wind speed and the excitation of the first azimuth flexible mode (1.66 Hz). The torque spectra show additional excitation of the higher-frequency (4.23 Hz) azimuth mode.

Figure 9 shows the dependency of the azimuth encoder and azimuth torque power spectrum on wind speed, when the yaw angle is 90 deg and the elevation angle is 10 deg. For low frequencies, this side wind has almost the same effect for 37 and 45 km/hr (23 and 28 mph) speeds.

Figure 10 presents the azimuth encoder and torque spectra for a 180-deg yaw angle, a 60-deg elevation angle, and a 42 km/hr (26 mph) wind. For this angle, the torque spectrum shows, besides the already observed azimuth modes (1.66 and 4.23 Hz), the first elevation mode of 1.95 Hz excited.

Figure 11 presents the spectra for a 180-deg yaw angle, a wind speed of 40 km/hr (25 mph), and elevation angles of 20 and 78 deg. For low frequencies, the spectra for a 20-deg elevation are larger than the spectra for a 78-deg elevation angle, while for high frequencies the situation is reversed.

The spectra show that most of the wind energy is accumulated in the low frequencies; hence, an improved controller can compensate for this larger portion of the wind disturbance. They also show that the principal azimuth and elevation flexible modes are significantly excited, followed by the azimuth 4.23-Hz mode.

⁵ H. Ahlstrom and J. Mellstrom, "Antenna Friction Unbalance Measurements," JPL Interoffice Memorandum 3324-91-012 (internal document), Jet Propulsion Laboratory, Pasadena, California, March 6, 1991.

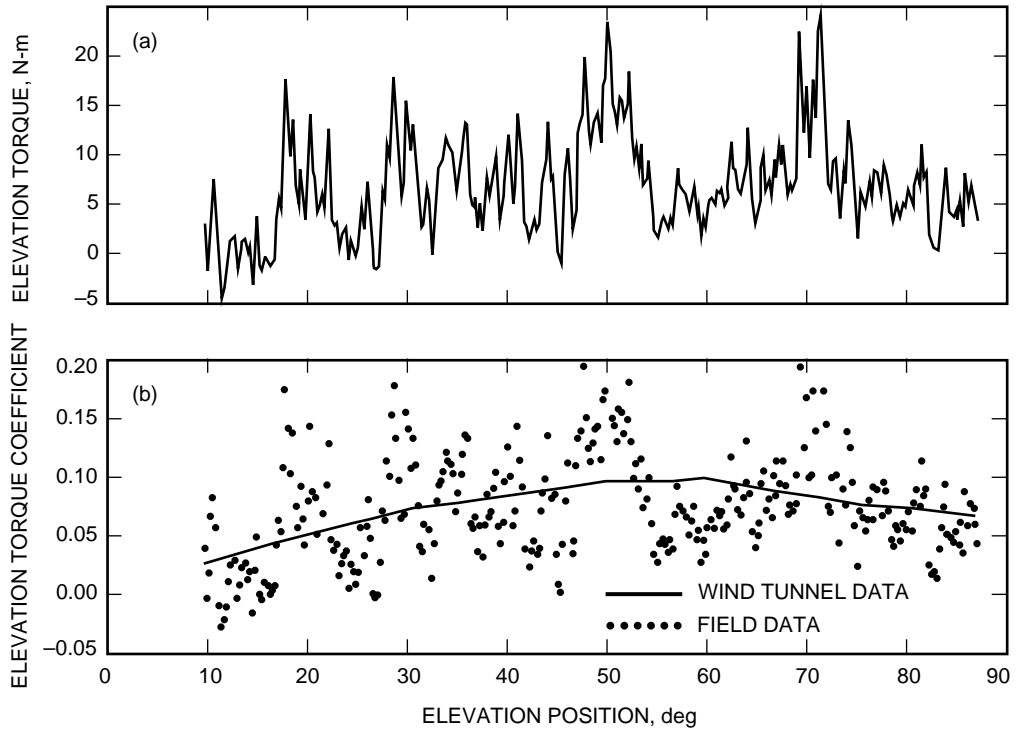


Fig. 6. Elevation angle 60 deg: (a) elevation torque and (b) elevation torque coefficient from wind tunnel data and field data.

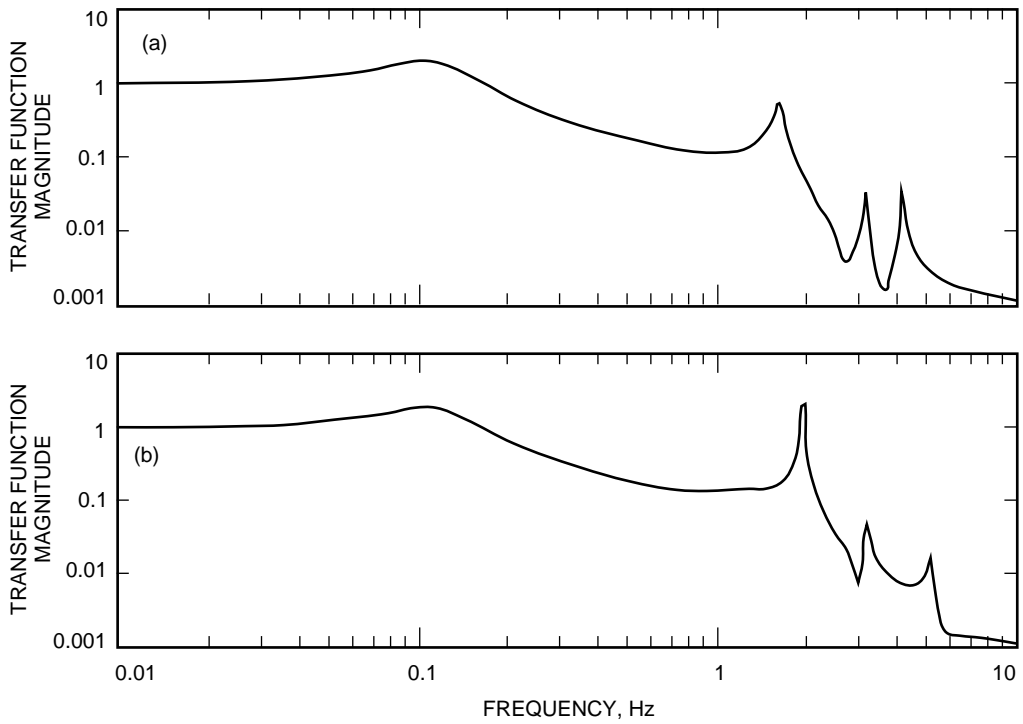


Fig. 7. Magnitudes of the transfer function of the DSS-13 servo: (a) in azimuth and (b) in elevation.

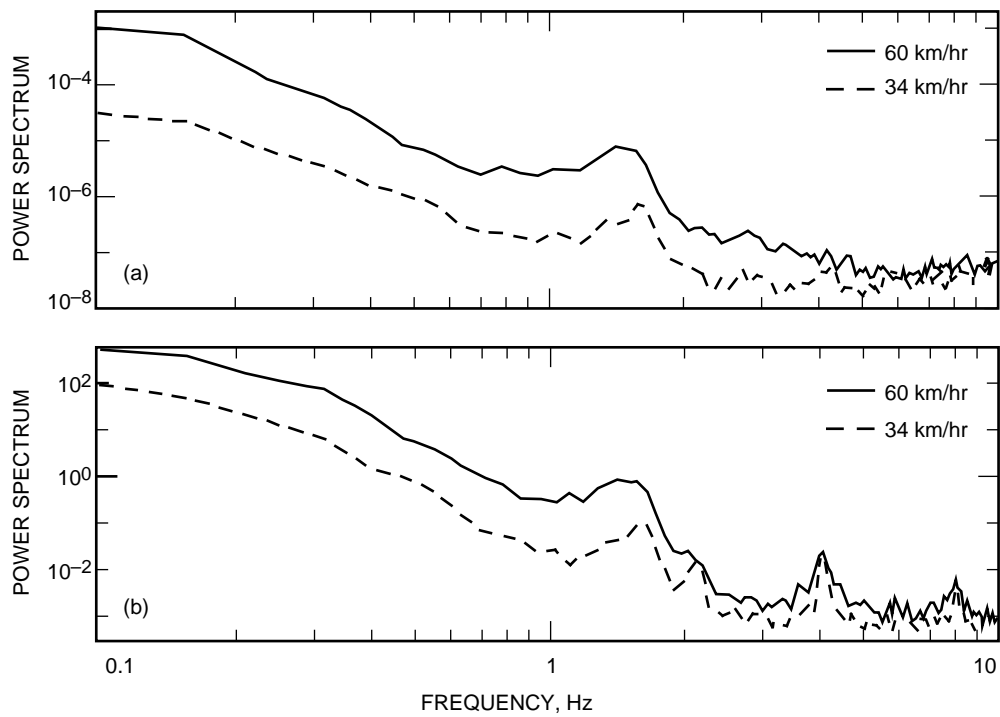


Fig. 8. Power spectra for yaw angle 180 deg and elevation angle 10 deg: (a) azimuth encoder and (b) azimuth torque.

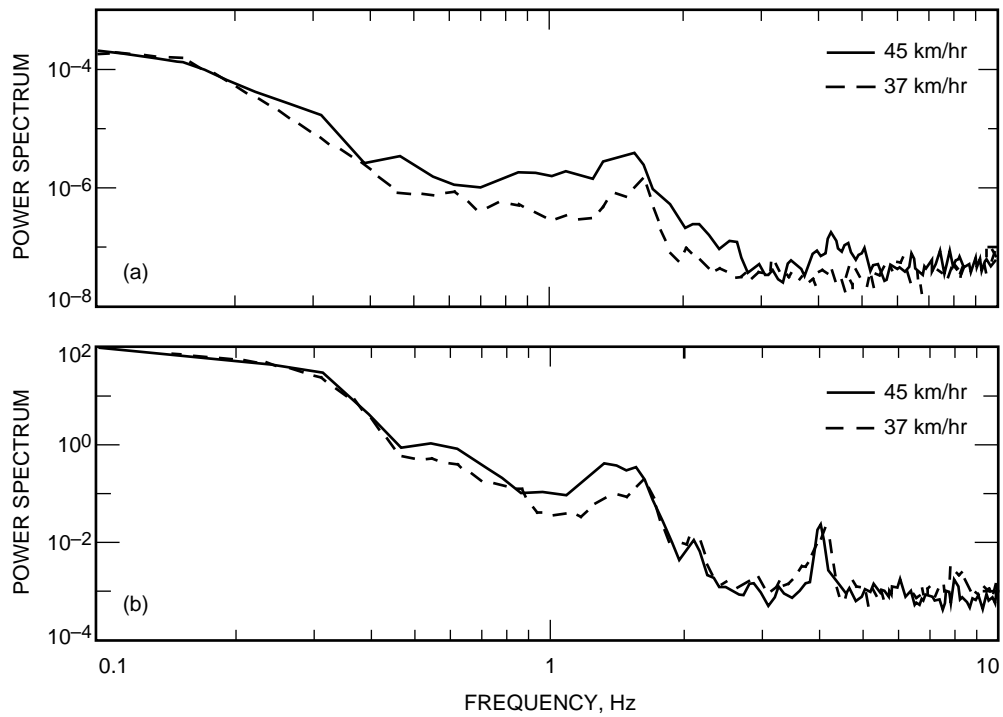


Fig. 9. Power spectra for yaw angle 90 deg and elevation angle 10 deg: (a) azimuth encoder and (b) azimuth torque.

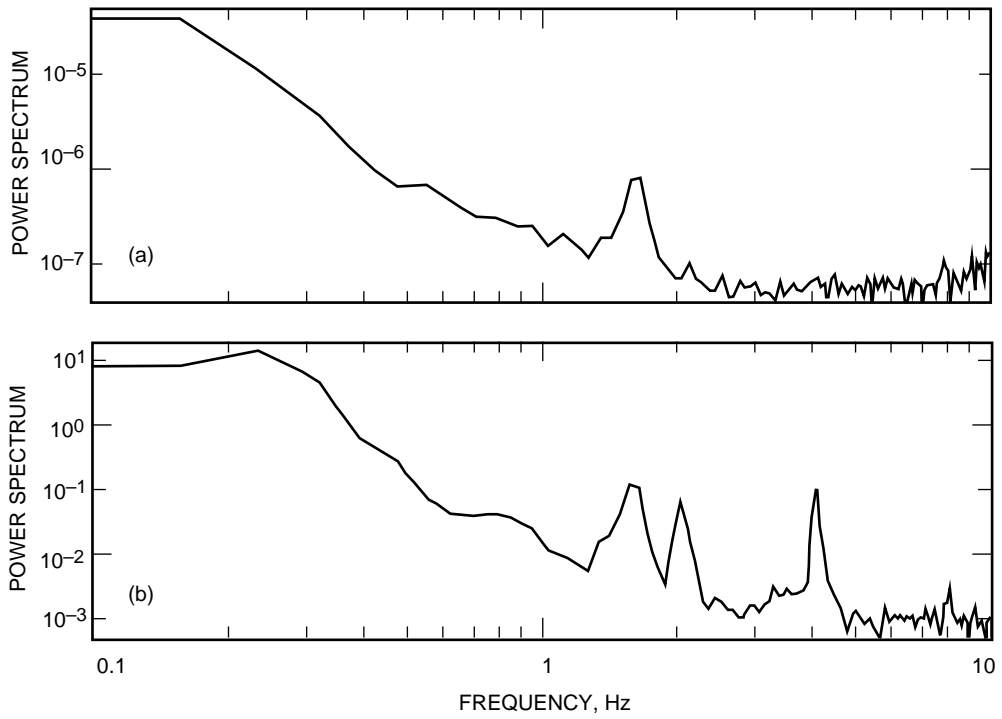


Fig. 10. Power spectra for yaw angle 180 deg and elevation angle 60 deg: (a) azimuth encoder and (b) azimuth torque.

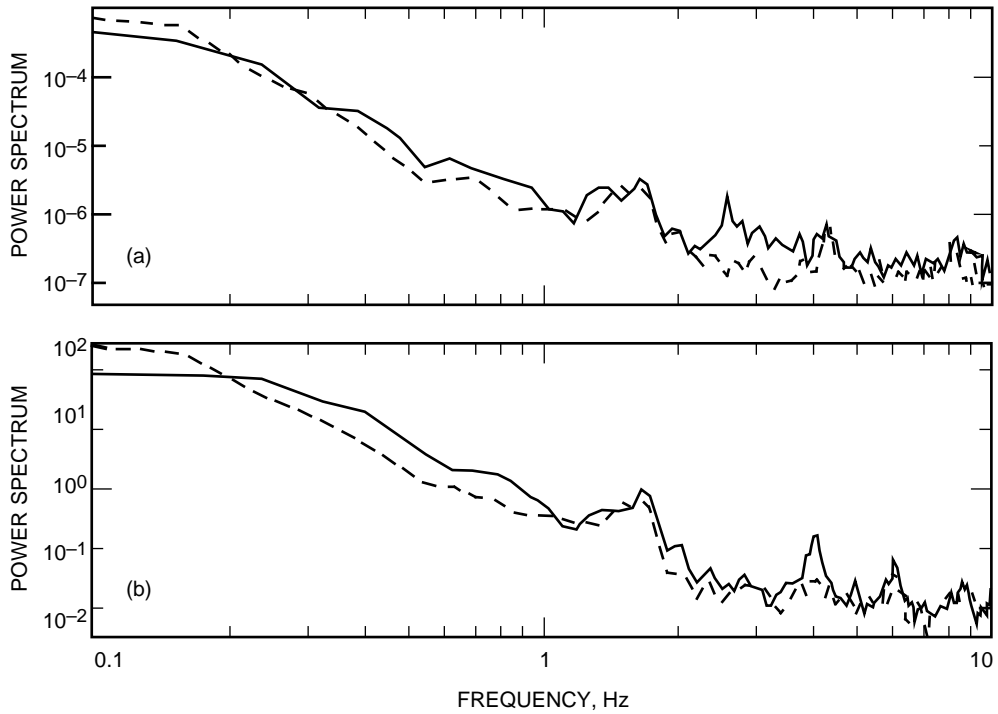


Fig. 11. Power spectra for yaw angle 180 deg and elevation angle 78 deg (solid line) and 20 deg (dashed line): (a) elevation encoder and (b) elevation torque.

IV. Conclusions

The comparison of selected field measurements with the wind tunnel data shows good agreement for the steady-state winds. The differences between the wind steady-state torque coefficients at the DSS-13 antenna and the wind tunnel data were less than 10 percent of the field-measured coefficients. The wind gusting action on the antenna, characterized by the power spectra of the antenna encoder and the antenna torques, showed the wind gusting primarily affects the antenna principal modes.

References

- [1] W. Gawronski and B. Bienkiewicz, "Pointing-Error Simulations of the DSS-13 Antenna Due to Wind Disturbances," *The Telecommunications and Data Acquisition Progress Report 42-108*, vol. *October–December 1991*, Jet Propulsion Laboratory, Pasadena, California, February 15, 1992.
- [2] W. Gawronski and J. A. Mellstrom, "Beam-Waveguide Antenna Servo Design Issues for Tracking Low Earth-Orbiting Satellites," *The Telecommunications and Data Acquisition Progress Report 42-115*, vol. *July–September 1993*, Jet Propulsion Laboratory, Pasadena, California, pp.135–152, November 15, 1993.